Investigating Correlations Between Day-to-Day Variability in Pre-Reversal Enhancement in Equatorial Plasma Drifts and Neutral Winds

Fatima Yousuf[1], Brian Harding[1], Claire Gasque[1], Colin Triplett[1], Thomas Immel[1], Astrid Maute[2], Yen-Jung Joanne Wu[1], Gilda Gonzalez[1]

[1] Space Sciences Laboratory, University of California, Berkeley, CA, USA
[2] Leibniz Institute of Atmospheric Physics (IAP), Kühlungsborn, Germany

Background

- The Pre-Reversal Enhancement (PRE) is an enhancement of the eastward equatorial electric field near sunset, driven by the F-region neutral wind dynamo. Its strength has been linked equatorial plasma bubble occurrence, which degrade GPS and radio communications. **The drivers of the PRE's day-to-day variability remain uncertain.** A natural candidate is variations in the zonal neutral wind, a driver for the PRE mechanism [1].
  - Abadi et al. (2021) [2] found r = 0.42 between F-region zonal winds (~250 km) and PRE strength, but used measurements at a single location and neutral winds at a limited altitude range.
  - Ghosh et al. (2020) [3] used the GAIA model to show that F-region zonal winds at the PRE peak time are correlated with PRE strength ($r \approx 0.5$ above 300 km). However, this study was confined to a single location and relied entirely on simulation model output.
- **We investigate: (1) whether the magnitude of the PRE is correlated with the concurrent zonal neutral winds, and (2) whether day-to-day changes in PRE strength are correlated with day-to-day changes in concurrent zonal neutral winds. Both analyses are stratified by solar flux level.**

Data & Instrument

- We use ICON [4] measurements between 1 January 2020 and 24 November 2022
- We use version 6 plasma drifts from ICON IVM-A and version 6 neutral wind measurements from ICON MIGHTI.
- We use WACCM-X simulations to investigate how MIGHTI sampling gaps affect observed correlations. We interpolate simulation data to times, altitudes, latitudes, and longitudes sampled by ICON. We consider two cases of WACCM-X datasets:

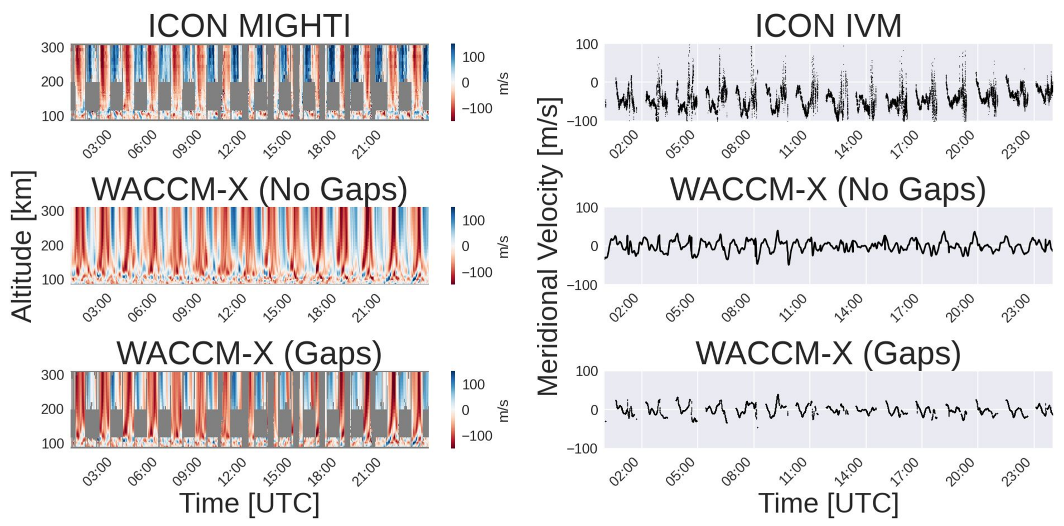

Figure 1. Example time series for January 6, 2020 illustrating the three dataset configurations. ICON and MIGHTI data (top row), WACCM-X without gaps (middle row), and WACCM-X with gaps (bottom row).

1) With gaps: only includes data at times/locations where the ICON data is flagged with the highest quality.
2) Without gaps: includes data at all times/locations sampled by ICON, irrespective of data quality flags.

Calculating the PRE Strength & Neutral Wind Conditions

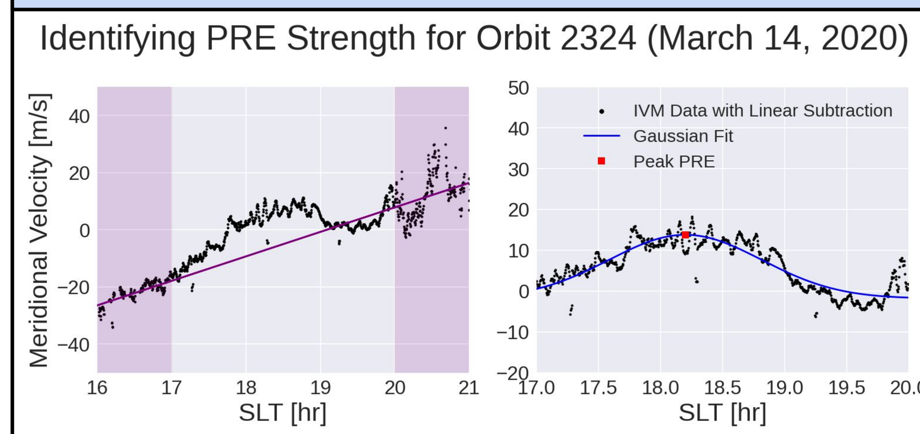

Figure 2. Left: Meridional drift (black) measured by IVM on March 14, 2020. Background linear fit (purple) using drift measurements during 16-17 SLT and 20-21 SLT Right: background-subtracted IVM meridional drift (black) and a Gaussian fit (blue). The strength of the PRE is quantified as the peak of the Gaussian fit, denoted with a red square.

For each ICON orbit crossing the magnetic equator at 17-20 SLT, we:

1) Subtract a background linear trend from the IVM meridional velocity
2) Fit a Gaussian to the background-subtracted meridional drift to calculate PRE strength [4].
3) Average MIGHTI zonal neutral winds in the same 0.25 hr SLT bin as the PRE peak.
4) Pair orbits 24 ± 1.5 hrs apart at the same magnetic longitude (within 10°). Compute ΔPRE and Δwind for each pair.
5) Separate by solar flux. Calculate correlations between PRE strength and winds. Apply false discovery rate corrections to p-values [5].

How Quickly Does the PRE Decorrelate?

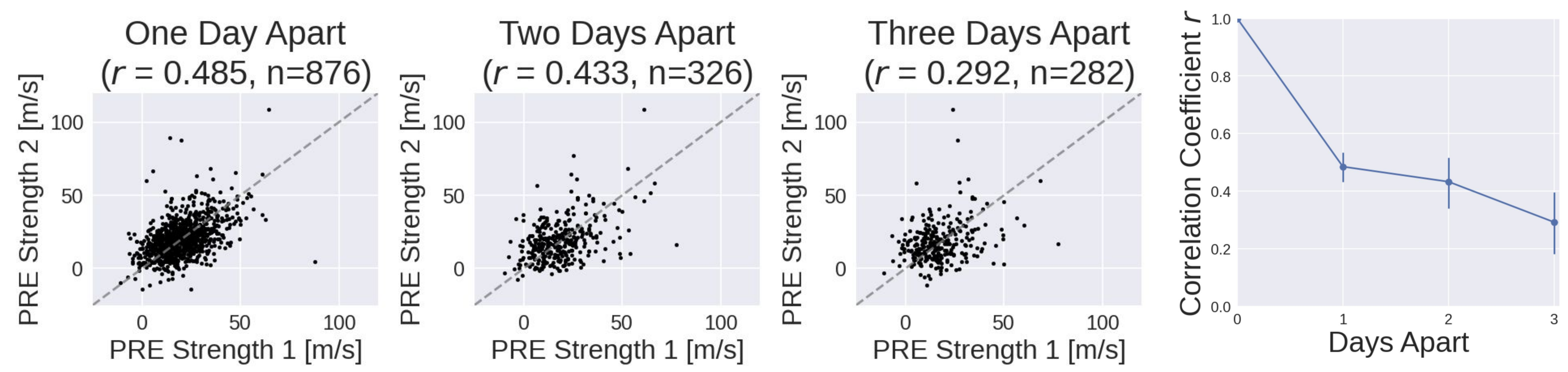

Figure 3. We identify pairs of ICON orbits that cross the magnetic equator at approximately the same location (within 10°) between 17-20 SLT about one, two, and three days apart from each other. We calculate the PRE strength and plot the PRE strengths of each orbit in each pair against each other.

The PRE strength decorrelates from r=1 *at* $\Delta t = 0$ *to* r = 0.485 *at* $\Delta t = 1$ *day* to r = 0.292 *at* $\Delta t = 3$ *days*, demonstrating the **PRE exhibits day-to-day variability and is not dominated by climatological trends**.

How Quickly Do Neutral Winds Decorrelate?

Figure 4. We identify pairs of ICON orbits that cross the magnetic equator at approximately the same location (within 10°) between 17-20 SLT about one, two, and three days apart from each other. We average MIGHTI neutral winds measurements taken during those orbits between 18-18.25 SLT for three representative altitude bins.

F-region winds (r = 0.436 after 3 days) retain more coherence than E-region winds (r = 0.173).

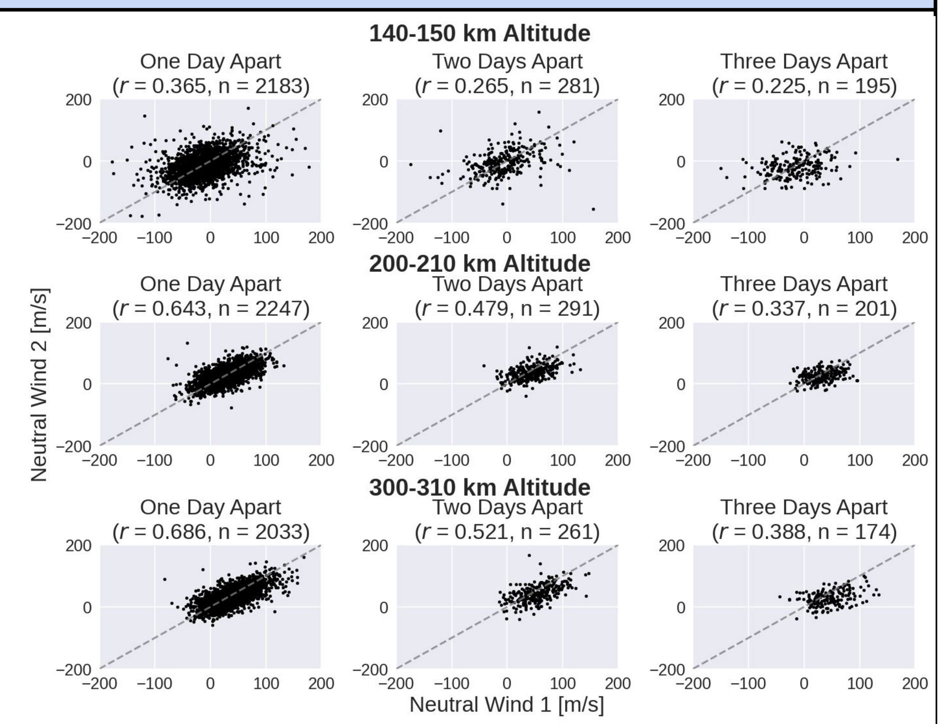

Results: Correlations Between the PRE Strength and Neutral Winds

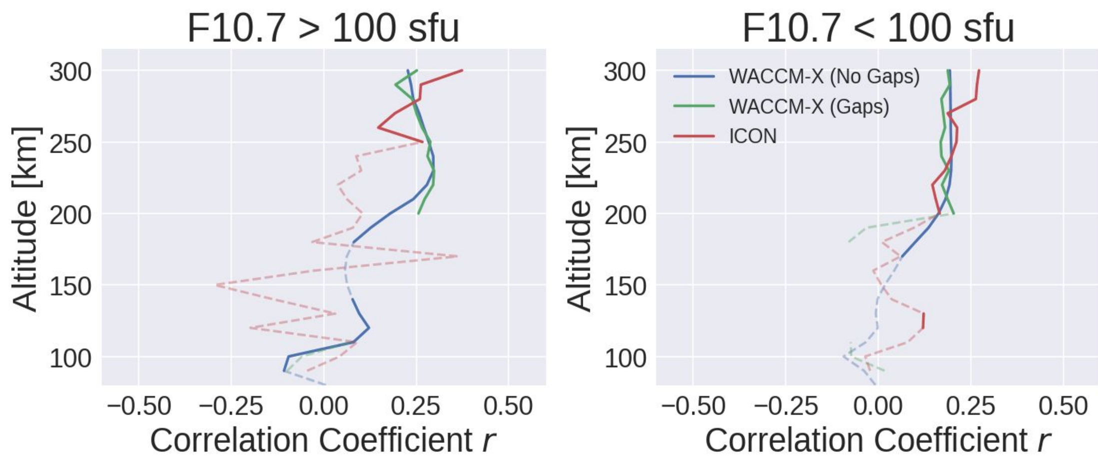

Figure 5. Correlations between PRE strength and concurrent zonal winds, stratified by solar flux. Solid lines indicate statistically significant correlations (FDR-corrected $p \leq 0.05$). Dashed lines do not pass statistical significance tests.

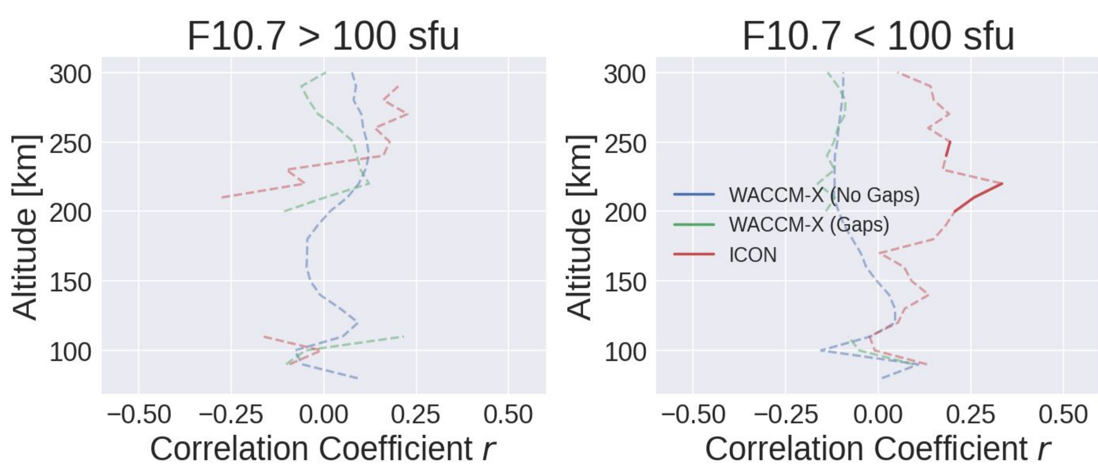

Figure 6. Correlations between day-to-day changes in the PRE strength and day-to-day changes in concurrent zonal neutral winds, stratified by solar flux. Solid and dashed lines are as in Figure 5.

Conclusions

The PRE decorrelates over 1-3 days (Fig. 3)
- r = 0.485 after 1 day
- r = 0.433 after 2 days
- r = 0.292 after 3 days

Direct correlations between PRE strength and zonal winds show stronger relationships (Fig. 5)
- Strongest during high solar activity
- ICON: r ≈ 0.374 at 300–310 km for F10.7 > 100

Neutral winds show similar decorrelation (Fig. 4)
- Comparable timescales over 1-3 days
- Upper F-region winds remain coherent longer

Day-to-day wind changes are weak predictors of day-to-day PRE changes (Fig. 6)
- ICON correlations are mostly positive, but few bins meet statistical significance criteria
- WACCM-X correlations rarely exceed $|r| \approx 0.2$

Neutral wind–PRE correlations are weak on a day-to-day difference basis, but emerge more strongly in direct correlations under high solar activity and high altitudes (>200km).

Future Work

Future work will
- Extend the analysis to other local time windows beyond the concurrent PRE peak bin. For example, testing whether winds 1–2 hours before the PRE peak are better predictors
- Screen for geophysical disturbances (substorms, high-speed solar wind streams, solar flares) to isolate the PRE response to neutral winds
- Explore nonlinear statistical methods (e.g. Spearman rank correlation or mutual information) to see if the wind–PRE relationship is better described nonlinearly

Acknowledgements

This work was supported by NSF AGS-2230365. ICON is supported by NASA's Explorers Program through contracts NNG12FA45C and NNG12FA42I. ICON-IVM and MIGHTI data can be retrieved from the Space Physics Data Facility [6][7]. F10.7 flux data were obtained from Space Weather Canada [8].

References

[1] Harding, B. J., Serrano, M. C., Gasque, L. C., Joanne Wu, Y., Maute, A., & Immel, T. J. (2025, January). Wind-driven variability in the prereversal enhancement of the equatorial vertical plasma drift: Climatologies observed by ICON. Journal of Geophysical Research: Space Physics, 130 (1). doi: 10.1029/2024ja033279385
[2] Abadi, P., Otsuka, Y., Liu, H., Hozumi, K., R. Martinigrum, D., Jamjareegulgarn, P., . . . Otadoy, R. (2021). Roles of thermospheric neutral wind and equatorial electrojet in pre-reversal enhancement, deduced from observations in southeast asia. Earth and Planetary Physics, 5 (5), 388–397. doi: 10.26464/epp2021049
[3] Ghosh, P., Otsuka, Y., Mani, S., & Shinagawa, H. (2020, July). Day-to-day variation of pre-reversal enhancement in the equatorial ionosphere based on gaia model simulations. Earth, Planets and Space, 72 (1). doi: 10.1186/s40623-020-01228-9
[4] Immel, T. J., Harding, B. J., Heelis, R. A., Maute, A., Forbes, J. M., England, S. L., et al. (2021). Regulation of ionospheric plasma velocities by thermospheric winds. Nature Geoscience, 14(12), 893–898. doi: 10.1038/s41561-021-00848-4
[5] Benjamini, Y., & Hochberg, Y. (1995). Controlling the false discovery rate: A practical and powerful approach to multiple testing. Journal of the Royal Statistical Society. Series B (Methodological), 57 (1), 289–300. Retrieved 2026-06-09, from http://www.jstor.org/stable/2346101467
[6] Heelis, R. A. (2023). Icon ion velocity meter (ivm) a data. Space Physics Data Facility. Retrieved from https://spase-metadata.org/NASA/NumericalData/ICON/IVM/L2/A/PT1S doi: 10.48322/2MV5-XY46
[7] Harding, B. J., Englert, C. R., Harlander, J. M., Marr, K. D., Makela, J. M., Brown, C. M., . . . Immel, T. J. (2023). Icon michelson interferometer for global high-resolution thermospheric imaging viewing direction a. Space Physics Data Facility. Retrieved from https://spase-metadata.org/NASA/NumericalData/ICON/MIGHTI/L2/A/Green/PT30S doi: 10.48322/07NF-QA27
[8] Space Weather Canada. (2026). Daily solar flux values. https://spaceweather.gc404 .ca/solar flux data/daily flux values/fluxtable.txt